Title
CONCENTRATION AND VELOCITY PROFILES IN A STEFAN DIFFUSION TUBE

Authors
Heinzelmann, Fred J.
Wasan, Darshanlal T.
Wilke, Charles R.

Publication Date
1963-08-01

UCRL-10421 Rev./

University of California

Ernest O. Lawrence Radiation Laboratory

CONCENTRATION AND VELOCITY PROFILES IN A STEFAN DIFFUSION TUBE

Berkeley, California

DISCLAIMER

UCRL-10421 Rev./

UNIVERSITY OF CALIFORNIA

Lawrence Radiation Laboratory
Berkeley, California

Contract No. W-7405-eng-48

CONCENTRATION AND VELOCITY PROFILES IN A STEFAN DIFFUSION TUBE

Fred J. Heinzelmann, Darshanlal T. Wasan, and Charles R. Wilke

August 1963

CONCENTRATION AND VELOCITY PROFILES IN A STEFAN DIFFUSION TUBE

Fred J. Heinzelmann, Darshanlal T. Wasan, and Charles R. Wilke

Lawrence Radiation Laboratory and Department of Chemical Engineering
University of California, Berkeley, California

ABSTRACT

The Stefan diffusion tube has been widely used as a means of determining vapor-phase diffusion coefficients. By this method the diffusion coefficient has been calculated on the assumption of plug-flow (flat) concentration and velocity profiles in the diffusion tube. These assumptions have been examined theoretically and experimentally in this study.

The theoretical study and the experimental results indicate that the concentration profile is flat across the diffusion tube. Velocity and concentration profiles were estimated by approximate analytical solutions of the diffusion-convection equations. The velocity profile is found to be developing from a flat one near the liquid surface to a parabolic one at the other end of the tube. However, it is shown theoretically that the shape of the velocity profile does not affect the mass flux provided the concentration profile is flat. Thus diffusion data that have been calculated from Stefan diffusion tube data with the plug flow approximation are substantially correct.

CONCENTRATION AND VELOCITY PROFILES IN A STEFAN DIFFUSION TUBE*

Fred J. Heinzelmann, Darshanlal T. Wasan, and Charles R. Wilke

Lawrence Radiation Laboratory and Department of Chemical Engineering
University of California, Berkeley, California

INTRODUCTION

The Stefan diffusion tube has been widely used for the determination of vapor-phase diffusion coefficients. The liquid to be vaporized is placed in the bottom of a vertical tube which is maintained at a constant temperature. A gas is passed over the top of the tube at a rate sufficient enough to keep the partial pressure of the vapor there at the value essentially corresponding to the initial composition of the gas but low enough to prevent turbulence. The mass flux is determined by weighing the tube during the quasi-steady state evaporation period. The vapor-phase diffusion coefficients are readily calculated from the mass flux and concentration gradient over the diffusion path with the assumption of plug flow in the tube. A critical review of the experimental technique has been presented by Lee and Wilke.[11]

The equations for isothermal diffusion are well known, having first been developed by Maxwell[10] and Stefan.[14,15] For the ith component, these equations have the form

$$-\frac{P}{RT}\frac{dy_i}{dx} = \sum_{j\neq i}^{n} \frac{N_i y_j - N_j y_i}{D_{ij}} \quad . \tag{1}$$

This equation, in the case of binary diffusion, which is the case of interest in this study, can be transformed into[16]

$$N_A = \frac{-D_{AB}P}{RT} \frac{dy_A}{dx} + (N_A + N_B)y_A. \qquad (2)$$

This equation defines the vapor-phase diffusion coefficient D_{AB}.[1]

With component B stagnant, i.e., $N_B = 0$, the equation becomes

$$N_A = \frac{-D_{AB}P}{RT} \frac{dy_A}{dx} + N_A y_A . \qquad (3)$$

The first term on the right-hand side is the contribution of equimolal diffusion; the second term is interpreted as the contribution to the flux of A due to the bulk flow set up by the diffusion. Integration of Eq. (3), assuming D_{AB} constant, gives[16]

$$N_A = \frac{D_{AB}P \Delta p}{RT\Delta x (p_f)} , \qquad (4)$$

where (p_f) is the diffusion-film-pressure factor. It is defined as

$$p_f = \frac{(P-p_S) - (P-p_0)}{\ell n \frac{P-p_S}{P-p_0}} .$$

Equation (4) is used to calculate diffusion coefficients from data obtained in the Stefan tube apparatus.

Inherent in the integration of Eq. (3) is the assumption that no radial concentration gradients exist in the Stefan tube. This assumption has not previously been verified. The study presented here involves a theoretical analysis of the diffusion system and an experiment designed to determine whether or not the flat-profile assumption is valid.

Theoretical Analysis

Consider the diffusion system shown in Fig. 1. Liquid A is evaporating into a stagnant column of gas B. At the liquid-gas interface (x = 0) the gas phase concentration of A, corresponding to equilibrium with the liquid, is denoted by C_S.

At the tope of the tube (x = L) a stream of gas B flows past slowly. The system is kept at constant temperature and pressure. At steady state there is a net flux of component A away from the evaporating surface and component B is stagnant.

The basic differential equations of momentum and mass are used as a starting point in establishing the concentration distribution as a function of the radial and axial directions. In the absence of an axial pressure gradient and the radial and azimuthal velocities we may write the x component of the steady state momentum equation, in cylindrical coordinates for homogeneous fluid as[2]

$$u \frac{\partial u}{\partial x} = \nu \frac{1}{r} \frac{\partial}{\partial r} \left(r \frac{\partial u}{\partial r} \right) + \nu \frac{\partial^2 u}{\partial x^2} . \qquad (5)$$

The assumption that $\frac{\partial p}{\partial x}$ is negligible is demonstrated by calculations in the appendix.

The corresponding steady-state diffusion equation for component A with a constant diffusion coefficient and density is[3]

$$u \frac{\partial C_A}{\partial x} = D \frac{1}{r} \frac{\partial}{\partial r} \left(r \frac{\partial C_A}{\partial r} \right) + D \frac{\partial^2 C_A}{\partial x^2} . \qquad (6)$$

Equation (6) results from the application of conservation of mass and Fick's first law.

Now consider the boundary values of the system.

1. The concentration of A at the liquid-gas interface is constant. Hence

$$C_A = C_S \text{ , a constant at } x = 0 \text{ for all } r.$$

2. The concentration of A at the top of the tube is zero. Hence

$$C_A = 0 \quad \text{at} \quad x = L \text{ for all } r.$$

3. The concentration profile is symmetrical about the x axis. Hence

$$\frac{\partial C_A}{\partial r} = 0 \quad \text{at } r = 0 \text{ for all } x.$$

4. There is no transfer from the walls of the tube into the gas. Hence

$$\frac{\partial C_A}{\partial r} = 0 \quad \text{at } r = r_0 \text{ for all } x.$$

5. There is no slip at the wall. Hence

$$u = 0 \quad \text{at } r = r_0 \text{ for all } x.$$

6. The velocity profile is symmetrical about the x axis. Hence

$$\frac{\partial u}{\partial r} = 0 \quad \text{at } r = 0 \text{ for all } x.$$

7. At the evaporating surface the diffusion velocity is related to the concentration gradient of the diffusing species by

$$u = -\frac{D}{C_B} \frac{\partial C_A}{\partial x} \quad \text{at } x = 0 \text{ for all } r.$$

The above equations assume that the mass average velocity is equal to the mole average velocity. This is true only when the molecular weight of A equals that of B. However, for low mass-transfer rates the assumption introduces little error and is satisfactory.

Since the form of the hydrodynamic velocity, u, in the tube is not known, several approximations are made and discussed here. First an average uniform hydrodynamic velocity u_0 over the tube cross section is assumed, and the solution to the diffusion equation (6) is achieved.

The solution of the diffusion equation (6) that satisfies the boundary conditions 1, 2, 3 and 4 is

$$C_0 = C_S \left[\frac{1 - \exp[u_0/D)(L-x)]}{1 - \exp[(u_0/D)L\ ]} \right] . \qquad (7)$$

Where u_0 can be determined by boundary condition 7, as

$$u_0 = - \frac{D}{C_B} \left(\frac{\partial C_0}{\partial x} \right)_{x=0} = \frac{D}{L} \ln\left(1 + \frac{C_S}{C_B}\right) .$$

Equation (7) is equivalent to Eq. (4) and both can be used to calculate either the mass flux or the concentration profile.

Now a new velocity distribution is assumed, of the form

$$u = u_0 + u_1 \qquad (8)$$

where $u_1(x,r)$ represents a perturbation in the previously assumed uniform hydrodynamic velocity, u_0 .

Substituting Eq. (8) into (5) and neglecting the second order terms the equation to be solved is

$$u_0 \frac{\partial u_1}{\partial x} = \nu \left[\frac{\partial^2 u_1}{\partial r^2} + \frac{1}{r} \frac{\partial u_1}{\partial r} + \frac{\partial^2 u_1}{\partial x^2} \right] . \qquad (9)$$

The diffusion system under consideration is characterized by very slow motion flow. Since the inertia forces are proportional to the square of the velocity, whereas the viscous forces are proportional to its first power, the inertia term may be neglected* as suggested by Schlichting,[13] and Eq. (9) rearranges into

$$\nu \left[\frac{\partial^2 u_1}{\partial r^2} + \frac{1}{r} \frac{\partial u_1}{\partial r} + \frac{\partial^2 u_1}{\partial x^2} \right] = 0 . \qquad (10)$$

Since u_0 is a constant, Eq. (10) can be written as

$$\frac{\partial^2 u}{\partial r^2} + \frac{1}{r} \frac{\partial u}{\partial r} + \frac{\partial^2 u}{\partial x^2} = 0. \qquad (11)$$

The boundary conditions are

1. No slip at the wall, or

$$u = u_1 + u_0 = 0 \qquad \text{at } r = r_0 \text{ for all } x.$$

2. The perturbation, u_1, must be zero at $x = 0$:

$$u_1 = 0 \qquad \text{at } x = 0 \text{ for all } r.$$

3. Since the system is axially symmetric,

*Since the axial inertial term is negligible it follows that the radial velocity which was neglected in formulating Eq. (5) is also neglibible.

$$\frac{\partial u}{\partial r} = 0 \qquad \text{at} \quad r = 0 \text{ for all } x.$$

4. The last boundary condition is obtained from the equation of continuity. At $x = 0$ the radial velocity is zero. Thus

$$\frac{\partial u}{\partial x} = 0 \quad \text{at } x = 0 \text{ for all } r.$$

The equation may now be solved by the method of a Separation of Variables. Assume that the solution of Eq. (11) is of the form

$$u = X(x)\, R(r); \tag{12}$$

when Eq. (12) is substituted in Eq. (11), there result two differential equations,

$$\frac{d^2X}{dx^2} - \frac{\alpha^2}{\nu} X = 0, \tag{13}$$

and

$$\frac{d^2R}{dr^2} + \frac{1}{r}\frac{dR}{dr} + \frac{\alpha^2}{\nu} R = 0 , \tag{14}$$

where α is a constant to be determined by the boundary conditions. The solution of Eq. (13) is

$$X = A \cos \sqrt{\frac{\alpha^2}{\nu}}\, x + B \sin \sqrt{\frac{\alpha^2}{\nu}}\, x . \tag{15}$$

Equation (14) is one form of Bessel's equation, and has solutions of the form

$$R = A' J_0 \left(\sqrt{\frac{\alpha^2}{\nu}}\, r\right) + B' Y_0 \left(\sqrt{\frac{\alpha^2}{\nu}}\, r\right), \qquad (16)$$

where A, A', B, and B' are constants to be determined by the boundary conditions. J_0 and Y_0 are zero-order Bessel functions of the first and second kinds. Applying boundary condition 3 gives $B' = 0$, and Eqs. (15) and (16) are combined to obtain the solution for u:

$$u = \left(A \cos \sqrt{\frac{\alpha^2}{\nu}}\, x + B \sin \sqrt{\frac{\alpha^2}{\nu}}\, x\right) J_0\left(\sqrt{\frac{\alpha^2}{\nu}}\, r\right). \qquad (17)$$

The application of boundary condition 1 requires a slight modification of the definition of u_0. Initially u_0 had been defined as being constant over the whole cross-sectional area. However, u_0 must be zero at the wall ($r = r_0$). Thus, for u_0 one can write

$$u_0 = \sum_n E_n J_0 \left(\beta_n \frac{r}{r_0}\right), \qquad (18)$$

where the E_n's are chosen so that u_0 has a constant value for all r except for $r = r_0$, where $u_0 = 0$. Then, when boundary condition 1 is applied both u_1 and u_0 are zero at $r = r_0$. The values of E_n are found through the orthogonality relationships.

Using boundary condition 1 on Eq. (17) requires $\sqrt{\frac{\alpha^2}{\nu}}\, r_0 = \beta_n$, which is a root of J_0. Hence

$$u = u_1 + u_0 = \left(A_n \cos \beta_n \frac{x}{r_0} + B_n \sin \beta_n \frac{x}{r_0}\right) J_0 \left(\beta_n \frac{r}{r_0}\right). \qquad (19)$$

Applying boundary condition 4 requires $B_n = 0$.

Therefore

$$u_1 = - u_0 + A_n \cos \beta_n \frac{x}{r_0} J_0 \left(\beta_n \frac{r}{r_0} \right) . \qquad (20)$$

Now, applying boundary condition 2, one has

$$u_1 \Big|_{x = 0} = 0 = - u_0 + \sum_n A_n J_0 \left(\beta_n \frac{r}{r_0} \right) . \qquad (21)$$

Substituting Eq. (18) for u_0 and comparing terms shows

$$E_n = A_n .$$

Hence

$$u = \sum_n E_n \cos \beta_n \frac{x}{r_0} J_0 \left(\beta_n \frac{r}{r_0} \right) . \qquad (22)$$

The values of E_n are found through the orthogonality relationships of the Bessel function as[5]

$$E_n = \frac{2u_0}{\beta_n J_1(\beta_n)} \qquad (23)$$

Solution of the Concentration Distribution

The concentration distribution is calculated by using the velocity distribution given by Eq. (22) in the diffusion equation (6). Assume now a perturbation, C_1, in the concentration such that

$$C = C_0 + C_1 , \tag{24}$$

where C_0 is given by Eq. (7). Substituting Eqs. (8) and (24) into Eq. (6) and after neglecting the second order terms the equation to be solved is

$$D \frac{\partial^2 C_1}{\partial x^2} - u_0 \frac{\partial C_1}{\partial x} + D \left(\frac{\partial^2 C_1}{\partial r^2} + \frac{1}{r} \frac{\partial C_1}{\partial r} \right) = u_1 \frac{\partial C_0}{\partial x} . \tag{25}$$

Equation (25) is to be solved with the boundary conditions

1. $C_1 = 0$ at $x = 0$, for all r,

2. $C_1 = 0$ at $x = L$, for all r,

3. $\frac{\partial C_1}{\partial r} = 0$ at $r = 0$, for all x,

4. $\frac{\partial C_1}{\partial r} = 0$ at $r = r_0$ for all x.

Boundary condition 1 results because the perturbation must be zero initially. Condition 2 follows from the statement of the problem, since C is given as zero at $x = L$, and C_0 is also zero at $x = L$. Boundary conditions 3 and 4 result, respectively, from the symmetry of the problem and from the impermeability of the wall to mass flow.

From boundary conditions 3 and 4 one is led to try a solution of the form

$$C_1 = \sum_k a_k(x)\, J_0\left(\lambda_k \frac{r}{r_0}\right) , \tag{26}$$

where λ_k is a root of J_1.

Substituting Eq. (26) into (25) and using the orthogonality condition of the Bessel function one gets

$$K_m a''_m(x) - L_m a'_m(x) - M_m a_m(x) = \sum_n g_n f_n(x) , \tag{27}$$

where

$$K_m = D \frac{r_0^2}{2} J_0^2(\lambda_m) , \tag{28}$$

$$L_m = u_0 \frac{r_0^2}{2} J_0^2(\lambda_m) , \tag{29}$$

$$M_m = D \frac{\lambda_m^2}{2} J_0^2(\lambda_m) , \tag{30}$$

$$g_n = E_n \frac{C_S u_0}{D} J_1(\beta_n) J_0(\lambda_m) \left[\frac{r_0^2 \beta_n}{\beta_n^2 - \lambda_m^2}\right] \left[\frac{\exp(-u_0 L/D)}{1-\exp(-u_0 L/D)}\right] \tag{31}$$

and

$$f_n(x) = \cos \beta_n \frac{x}{r_0} \exp(u_0 x/D). \tag{32}$$

Since the boundary conditions on C_1 are homogeneous, the boundary conditions on a_m are homogeneous. That is

$$a_m = 0 \qquad \text{at} \quad x = 0 \tag{33}$$

$$a_m = 0 \qquad \text{at} \quad x = L . \tag{34}$$

First, Eq. (27) is solved by assuming it is homogenous, i.e., $g_n = 0$. Then

$$K_m a''_m(x) - L_m a'_m(x) - M_m a_m(x) = 0. \tag{35}$$

This is a homogeneous equation with constant coefficients, which has a solution

$$a_m(x) = S_m \exp(b_1 x) + T_m \exp(b_2 x) \tag{36}$$

where

$$b_1 = \frac{L + \sqrt{L^2 + 4KM}}{2K} \tag{37}$$

$$b_2 = \frac{L - \sqrt{L^2 + 4KM}}{2K} \tag{38}$$

The constants, b_1 and b_2, are also functions of m.

From the form of the driving function the particular solution of Eq. (27) is[12]

$$y_{m,n} = G_{m,n} e^{Ax} \cos\beta_n x + H_{m,n} e^{Ax} \sin B_n x , \tag{39}$$

where

$$A = \frac{u_0}{D} \quad ,$$

$$B_n = \frac{\beta_n}{r_0} \quad .$$

$$H_n = - g_n \left(\frac{\gamma}{\phi^2 + \gamma^2} \right)$$

$$G_n = g_n \left(\frac{\phi}{\phi^2 + \gamma^2} \right)$$

$$\phi = KA^2 - KB_n^2 - LA - M \quad ,$$

and

$$\gamma = LB_n - 2KAB_n$$

For convenience the m subscript has been dropped. However, it must be remembered that this is only the solution for a particular value of m.

The total solution for C_1 is then found by combining the homogeneous and the particular solutions. Then one obtains

$$C_1 = \sum_m J_0 \left(\frac{\lambda_m}{r_0} r \right) \left\{ S_m \exp(b_1 x) + T_m \exp(b_2 x) \right\} \qquad (40)$$

$$+ \sum_m J_0 \left(\frac{\lambda_m}{r_0} r \right) \exp(Ax) \left\{ \sum_n G_{m,n} \cos(B_n x) + H_{m,n} \sin(B_n x) \right\} .$$

Where S_m and T_m are determined by applying the boundary conditions 1 and 2 as

$$S_m + T_m = -\sum_n G_{m,n}$$

and

$$S_m \exp(m_1 L) + T_m \exp(m_2 L) + \exp(AL) \sum_n G_{m,n} \cos(\beta_n L) + H_{m,n} \sin(\beta_n L) = 0$$

Since these equations contain summations they cannot be solved easily to obtain explicit functions for S and T. To obtain these, one must put in numerical values for $G_{m,n}$ and $H_{m,n}$. Then C_1 is calculated from Eq. (40).

APPARATUS

The apparatus used in this study is shown schematically in Fig. 2. The diffusion system is substantially the same as that used in recent measurements of diffusion coefficients and is described in detail by Getzinger.[6] However, a probe and electronic recording equipment have been added to measure the concentration profile.

Diffusion System

The diffusion unit is shown schematically in Fig. 3. The air enters the diffusion unit through straightening vanes to eliminate turbulence before passing over the diffusion tube. The diffusion unit was constructed of brass. Leads are provided to connect the probe and the electrical measuring devices.

The diffusion tube itself was designed to give a diffusion area with 1 in. i.d. The diffusion tube was built with a step design. The bottom was 1-in. i.d. and the top a 1.50-in. i.d. to accommodate the probe. With the probe in place the top part also had a 1-in.i.d. providing a smooth diffusion tube.

The probe was not extended to the bottom of the diffusion tube, so that liquid was prevented from rising up between the probe and the diffusion tube wall by capillary action (preliminary experiments had shown this to be a problem).

With the probe in place, the actual diffusion area was an uniform 1-in. i.d. circular cross section. An aluminum sleeve was used over the bottom of the diffusion tube to get a uniform outside diameter of 1.535 in. This gave a tight fit within the diffusion-tube holder, providing good thermal contact.

The diffusion tube itself was constructed with a wall thickness of only 0.018 in. This made the assembly light enough to be weighed on the

analytical balance in the laboratory to determine the weight loss by evaporation during a run.

Measurements were made of the time required to reach thermal equilibrium in the system. After only 15 minutes the gas temperature as measured by a conventional mercury thermometer was found to be within 0.1°C of the bath temperatures.

Air enters the system at room temperature from compressed air cylinders through a three-stage pressure regulator. It is then dried with an isopropyl alcohol-dry ice trap and is then further dried with a 6-in. column of Drierite. After passage through a flowrator, it is heated by an electric heating element to about 32°C. The air is then passed through 40 feet of copper tubing immersed in a constant-temperature bath, where it is heated to 35.0±0.1°C, the temperature used in the experiments. The diffusion unit is also immersed in the constant-temperature bath to insure isothermal operation. After passing through the diffusion unit the air is exhausted through a blower to the outside.

The constant-temperature bath is a 12-in.-diameter by 16-in-deep Pyrex jar housed in a large wooden box insulated with Styrofoam. The bath temperature is maintained at 35.0±0.1°C by an electric heating element regulated by a mercury thermoregulator connected to a specially built controller. The temperature was chosen to give a reasonably high vapor pressure for the benzene, the liquid used in the experiment. The bath is agitated by a Variac-controlled variable-speed General Electric motor driving a specially built propeller.

Probe

To measure the concentration profiles in the diffusion tube semicircular probes were used. The principle of the probe operation is the same as that of a thermal-conductivity cell. The detailed study of the optimum probe design is given elsewher.[8] Because of the radial symmetry of the diffusion system these probes could be used to measure the radial concentration gradients. Three probes were constructed, each of different diameter. The dimensions are given in Table I. A picture of probe 1 is shown in Fig. 4.

Table I. Probe dimensions

Probe	Nominal diameter (in.)	Maximum deviation from diameter (in.)	Nominal resistance (ohms)
1	3/4	± 1/16	24
2	9/16	± 1/32	18
3	7/16	< ± 1/32	15

The probes were constructed with an aluminum ring as the primary support. The probe itself was constructed of 0.000475-in. diameter cleaned tungsten wire obtained from the Wah Chang Corp. of New York. Thin glass capillaries were used to support the probe wire and maintain its semicircular shape.

The probe was placed in the diffusion tube along with three 1-in.-high 1-in. aluminum rings. The vertical position of the probe was changed by moving its position among these rings. All these aluminum rings had a machined inner surface of 1 in. i.d. in order to provide a smooth diffusion tube.

EXPERIMENTAL PROCEDURE

Benzene was chosen to be the diffusing substance and air as the gaseous diffusion medium. These were selected because considerable diffusion data have been obtained for these components in the Stefan-tube apparatus. Also these components have considerably different thermal conductivities, thus giving a reasonably good probe sensitivity. The temperature of the system was chosen at 35°C to give a reasonable vapor pressure and thus a significant mass flux.

The air flow rate over the diffusion tube was chosen to give minimum end effects due to turbulence at the top of the diffusion tube, but high enough to insure that stagnation did not take place. Preliminary experiments indicated that the air flow rate for this system should be about 120 cc/min, giving a velocity of 4.65 cm/sec through the straightening vanes in the diffusion system. This is somewhat lower than the gas rate used in Stefan-tube studies by Getzinger.[6] A lower gas rate was required because of increased turbulence in the diffusion system due to the presence of the probe leads. The gas rate fixed the operating pressure at 1.6 to 2.0 in. of water above atmospheric pressure.

After the air flow rate was determined some runs were made on the system without the probe in place, in order to determine the characteristics of the system. After these runs were finished runs were made with the probe in place. Data were taken with each probe in three vertical positions. Probe resistances were measured by using a Wheatstone bridge and Brush amplifier and recorder to measure the bridge balance.

When measurements were made of the probes the time used was as short as possible, in order to avoid setting up convection currents in the system. Several readings were made of each run, since making good electrical contacts

proved to be a problem. The probes were calibrated in calibration cells with known gas compositions.

Benzene loss in the Stefan diffusion tube was determined by weighing the tube before and after each run. Weights were determined to the nearest 0.0001 g. While out of the system the tube was kept stoppered at all times to prevent evaporation of benzene. Liquid depth in the tube was determined from the weight of benzene. Most runs lasted more than 3 hours. A few runs were only 30 to 40 minutes. Although it has been estimated that equilibrium is reached in 15 minutes,[11] these shorter runs gave badly scattered points and were discarded.

RESULTS AND DISCUSSION

Theoretical Results

Velocity and concentration profiles were calculated from Eqs. (7), (22), and (40). Values of the velocity u were calculated at several values of x and r. The results are shown in Fig. 5. The velocity profile starts out flat at $x = 0$, and slowly develops into what is essentially a parabolic profile at $x = 13$.

Since only the first two eigenvalues were used in these calculations, the values calculated are not yet completely converged, especially at $r = 0$ and $r = r_0$. At each value of x however, the average velocity must be the same, since at steady state the mass flux is constant throughout the tube. This was taken into account in drawing the velocity profiles. The values $D = 0.11$ cm^2/sec, $L = 13$cm, and $u_0 = 0.00186$ cm/sec are used in the calculations.

The values of the profile of the ratio of the concentration perturbation C_1 to the surface concentration C_s calculated at several values of the radial and axial distances are shown in Table II. The values of C_1 in Table II are based only on a limited summation of the series in Eq. (40). The values given are only for $m = 1$ and for the first four terms in n. A check of the magnitude of the terms for $m = 2$ showed that its contribution was approximately 10% of the first. Thus, C_1 is given by a rapidly convergent series.

Table II. Profile of concentration perturbation, C_1, given as C_1/C_s

	r/r_0			
x	0	0.24	0.71	0.87
6	-2.7×10^{-5}	-2.2×10^{-5}	0.4×10^{-5}	1.0×10^{-5}
13	0	0	0	0

Since the concentration profile is essentially that of C_0, there is no radial concentration gradient. Thus the flat concentration profile that was assumed in past interpretations of Stefan-tube data was correct, although there is not a flat velocity profile.

Now consider a diffusion tube with no radial concentration gradient but with some radial velocity distribution. Component A is diffusing through stagnant component B. In a thin cylindrical section, which has a constant velocity $u(r)$, the mass flux is given by

$$N_A = -D \frac{\partial C_A}{\partial x} + u(r)C_A. \qquad (41)$$

This is equivalent to Eq. (3). The total mass transfer is found by integrating over all values of r, or

$$J_T = \int_0^{r_0} N_A 2\pi r dr = 2\pi \int_0^{r_0} \left(-D \frac{dC_A}{dx}\right) r dr + 2\pi \int_0^{r_0} C_A u(r) r dr. \quad (42)$$

Since C_A is not a function of r, one gets

$$J_T = -D \left(\frac{\partial C_A}{\partial x}\right) \pi r_0^2 + u_0 \pi r_0^2 C_A \quad (43)$$

$$N_A = \frac{J_T}{\pi r_0^2} = -D \frac{\partial C_A}{\partial x} + u_0 C_A. \quad (44)$$

Equation (44) is the same equation one gets by assuming plug concentration and velocity profiles. This can be integrated to give Eq. (4).

Experimental Verification

The concentration profile measured by the probes is shown on Fig. 6 and summarized on Table IV. One can see that within the experimental error there is no radial concentration gradient.

The concentration gradient in x is of interest, since the values for large x (near the top of the tube) fall on the theoretical line but the points nearest the bottom of the tube indicate a considerably higher concentration than expected.

These points were rechecked and consistently gave the same results. Runs were made in which the probe measurements were made in air saturated with benzene by shutting off the system air flow. When the air flow was

started again and the system had reached equilibrium these high values were again obtained.

Diffusion coefficients were also calculated from the data. The true diffusion coefficient, corrected for end effects, was found to be 0.097 cm^2/sec. This value is somewhat lower than the value of 0.103 cm^2/sec obtained from the measurements by Lee and Wilke[11] corrected to our conditions. Since some inaccuracies might be expected in our experiment because of interference by the probes, the former measurements are considered preferable. The detailed experimental data are available elsewhere.[8]

The correction for end effects, Δx, was found to be 2.04 cm. This is quite large, and offers a possible explanation for the unexpectedly high concentration values near the bottom of the diffusion tube. If this whole end correction is applied to the bottom of the tube, then the predicted concentration profile and the data points are as shown on Fig. 7. The data at the bottom of the table are now much closer to the expected line, but the data at larger values of x now show some deviation from the predicted values. However, on the average, this does give a better fit to the data.

A possible cause of the large end effect at the bottom of the tube may be found in the diffusion thermo effect, according to which a temperature gradient is set up by a concentration gradient. This effect has been observed experimentally, and temperature differences of several degrees centigrade may be set up.[9]

In a binary mixture with a diffusion flow of component 1 there exists a heat flow

$$J_H = -\alpha' knT \text{ grad } N', \qquad (45)$$

where n is the total concentration of molecules 1 and 2, and N' is the mole fraction of molecule 1. The diffusion thermo-effect coefficient, α', for ideal mixtures is related to the thermal diffusion constant, α, by[7]

$$\alpha' = -D\alpha.$$

Since benzene is the larger and heavier molecule, one would expect α to be positive (i.e., benzene would diffuse toward the cooler end in thermal diffusion). Therefore α' would be negative. Thus, in Eq. (45), with grad N' also negative, the heat flux and the higher temperature would be near the bottom of the tube. Thus, one would have a cooler heavier gas on top of a warmer gas layer, starting convection currents. This could cause turbulence at the bottom of the tube and might explain the data points. Further work is required to confirm this.

CONCLUSIONS

A theoretical study of the Stefan diffusion-tube system indicates that

(a) there is no significant radial concentration gradient in the diffusion tube,

(b) the velocity profile, although flat at the liquid surface, becomes parabolic at large distances.

Experiment studies confirm that there is no significant concentration gradient within limitations of the measuring method. From these results it is concluded that equations developed from plug flow models for the Stefan tube could be used to calculate diffusion coefficients from the data.

APPENDIX

Estimation of Pressure Gradient in the Diffusion Tube

In developing the velocity and concentration equations it was assumed that the inertia terms and the pressure gradient term in the equations of motion (Eq. (9)) could be neglected. To check these assumptions an estimate was made, based on the calculated results, of the relative magnitude of these terms compared with the neglected term. They were found to be much smaller than the viscous term, as shown on Table III. Thus the assumptions were valid.

Table III. Calculated magnitude of the terms in the convection equation at x = 3.

Term	Magnitude of term
$\frac{\partial p}{\partial x}$	1×10^{-9}
$u \frac{\partial u}{\partial x}$	6×10^{-6}
$\nu \frac{\partial^2 u}{\partial x^2}$	1×10^{-3}

The term $\frac{\partial p}{\partial x}$ was evaluated by determining the derivative of the velocity at the wall.

This gave

$$\left.\frac{\partial u}{\partial r}\right|_{r=r_0} = \sum_k - \frac{2u_0}{r_0} \cos\left(\beta_k \frac{x}{r_0}\right).$$

The velocity gradient at the wall is related to the shear stress by

$$\tau = \mu \frac{du}{dr}$$

Now if we make a force balance, we obtain a relationship between $\frac{\partial p}{\partial x}$ and $\frac{\partial u}{\partial r}$:

$$\frac{dp}{dx} = -\frac{2}{r_0^2} \frac{\mu}{g_c} \sum_k u_0 \cos\left(\beta_k \frac{x}{r_0}\right).$$

This expression is then evaluated to give $\frac{dp}{dx}$.

A more rigorous method of solution that does not require the above assumptions would require a simultaneous solution of a fourth-order equation in the stream function and the diffusion Eq. (6) as outlined in reference 8. However, the solution is extremely difficult and probably can be obtained numerically only on a digital computer.

Table IV. Results obtained in determination of concentration profile

Probe 1

Run	19M	20M	21M	22M	38M
% Benzene	5.6	9.1	7.8	16.5	6.5
Probe depth (cm)	2.84	5.36	5.36	7.88	2.84
C/C_s	0.28	0.46	0.39	0.83	0.33
Fraction of diffusion distance	0.78	0.58	0.59	0.39	0.78

Probe 2

Run	15M	16M	17M
% Benzene	8.3	5.8	17.3
Probe depth (cm)	5.36	2.84	7.88
C/C_s	0.42	0.29	0.87
Fraction of diffusion distance	0.58	0.78	0.37

Probe 3

Run	25M	26M	27M
% Benzene	5.1	6.3	9.0
Probe depth (cm)	2.84	2.84	5.36
C/C_s	0.26	0.32	0.45
Fraction of diffusion distance	0.77	0.77	0.59

Probe 3

Run	29M	31M	33M
% Benzene	16.1	16.9	6.6
Probe depth (cm)	7.88	7.88	2.84
C/C_s	0.81	0.85	0.33
Fraction of diffusion distance	0.38	0.38	0.78

NOMENCLATURE

β	root of zero-order Bessel function of first kind
C	molar concentration
D	diffusion coefficient
J_0	zero-order Bessel function of the first kind
J_1	first-order Bessel function of the first kind
J_H	heat flux
J_T	total mass flow
λ	root of the first-order Bessel function of the first kind
N	mass flux
p	partial pressure
P	total pressure
R	gas constant
T	temperature
τ	shear stress
u	velocity in the x direction
v	velocity in the r direction
p_s	vapor pressure corresponding to surface temperature
p_0	vapor pressure of the inlet gas
ν	kinemtaic viscosity
μ	absolute viscosity

REFERENCES

* Work supported by the U. S. Atomic Energy Commission.

1. R. B. Bird, W. E. Stewart, and E. N. Lightfoot, Transport Phenomena (John Wiley and Sons, Inc., New York, 1960) p. 502.
2. Ibid., p. 85.
3. Ibid., p. 559.
4. Ibid., p. 131.
5. H. S. Carslaw and J. C. Jaeger, Conduction of Heat in Solids, 2nd Ed. (Oxford University Press, London, 1959) p. 196.
6. R. W. Getzinger, Steady-State Diffusion in Ternary Gas Mixtures, (M. S. Thesis), University of California, 1962.
7. R. Hasse, Z. Physik, 127, 1 (1950).
8. F. J. Heinzelmann, D. T. Wasan, and C. R. Wilke, UCRL-10421 (1962).
9. W. Jost, Diffusion in Solids, Liquids, and Gases, 3rd Printing (Academic Press, Inc., New York, 1960) p. 520.
10. J. C. Maxwell, Scientific Papers, Vol. 2 (Dover, New York, 1952).
11. C. Y. Lee and C. R. Wilke, Ind. Eng. Chem. 46, 2381 (1954).
12. H. S. Mickley, T. K. Sherwood, and C. E. Reed, Applied Mathematics in Chemical Engineering, 2nd Ed. (McGraw-Hill Book Company, Inc., New York, 1957) p. 153.
13. H. Schlichting, Boundary Layer Theory (McGraw-Hill Book Company, Inc., New York, 1955). p. 83.
14. J. Stefan, Sitzber. Akad. Wiss. Wien, Math.-naturw. Kl. 63, Abt II (1871).
15. Ibid., 65, Abt II, 323 (1872).
16. C. R. Wilke, Chem. Eng. Progr. 46, 95 (1950).

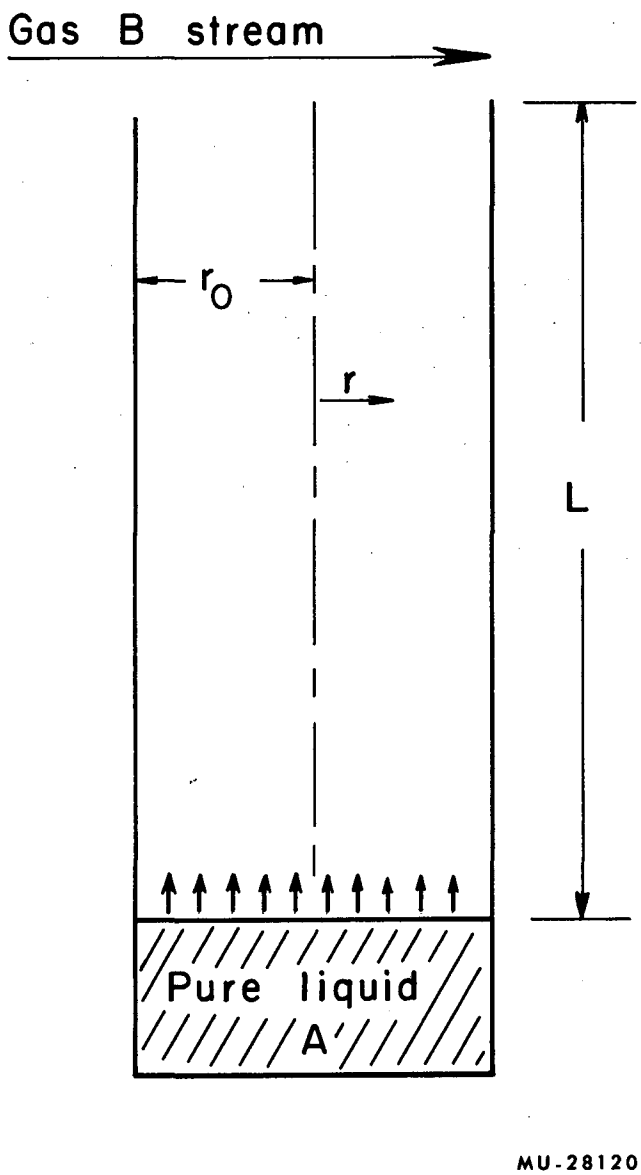

Fig. 1. Schematic diagram of the theoretical model.

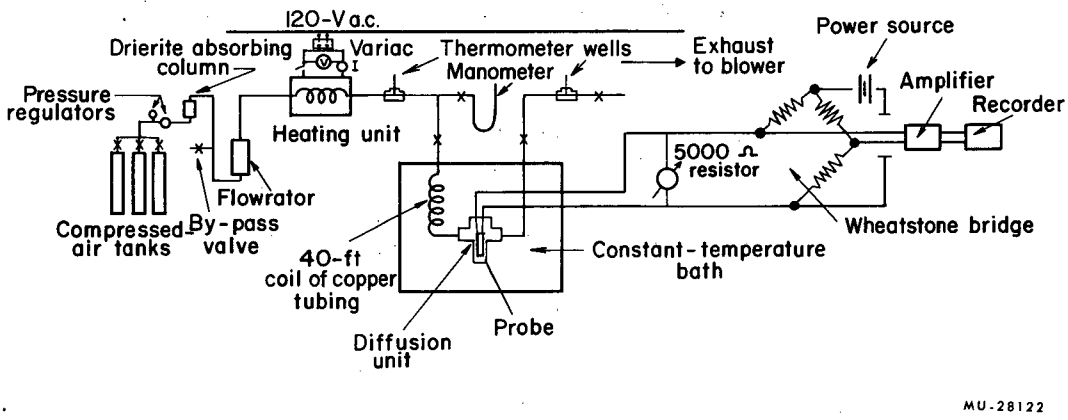

Fig. 2. Schematic diagram of the apparatus.

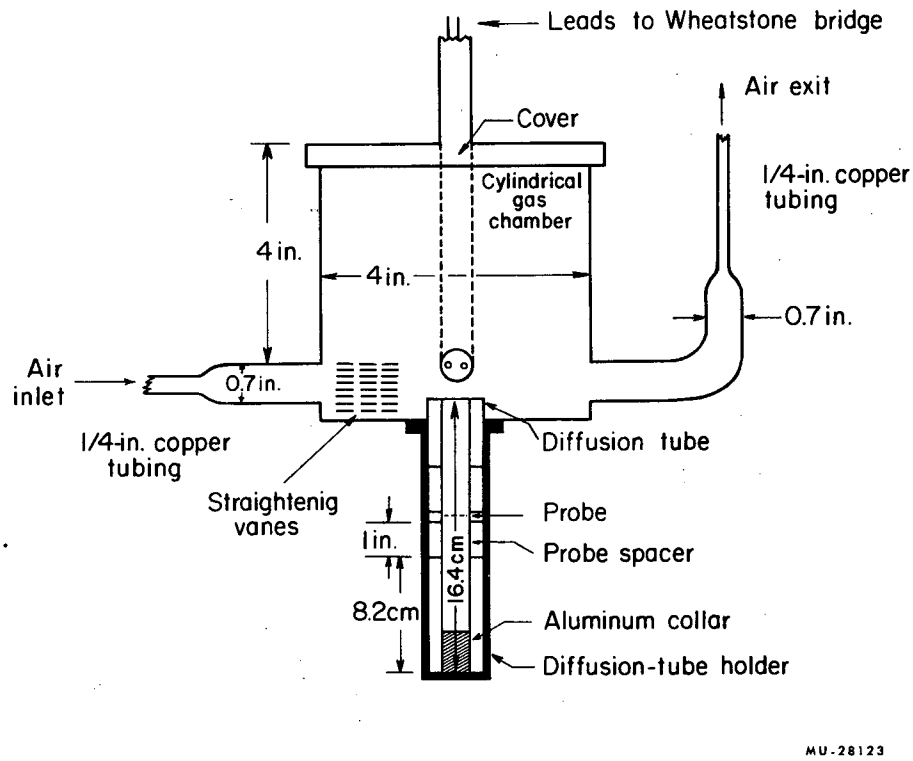

Fig. 3. Diffusion unit.

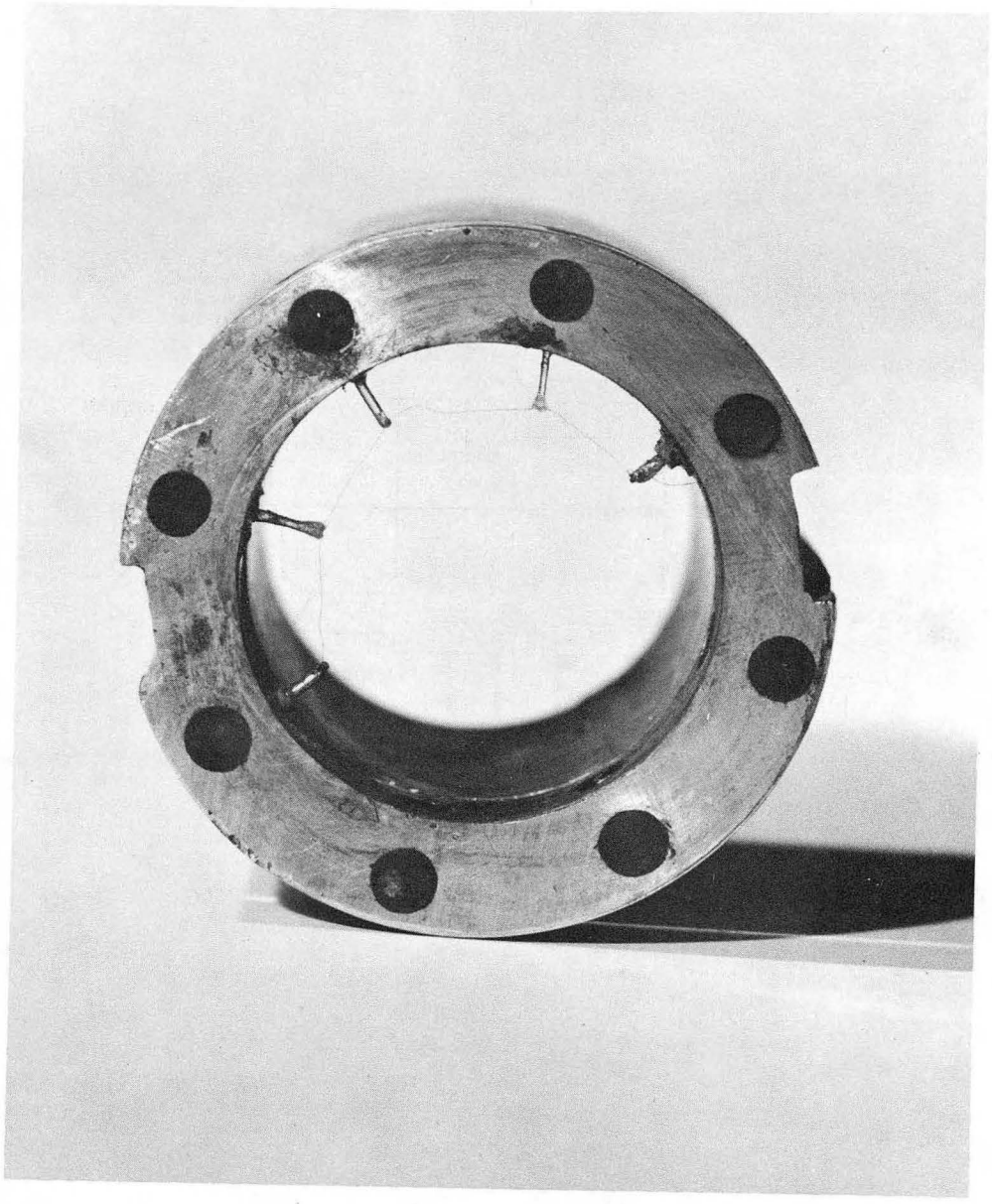

ZN-3358

Fig. 4. Probe 1.

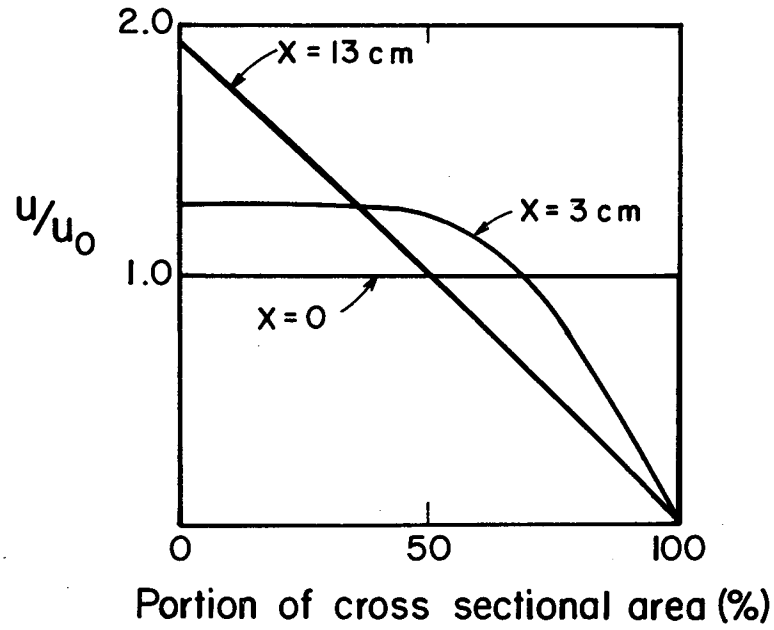

Fig. 5. Velocity profiles in a Stefan diffusion tube.

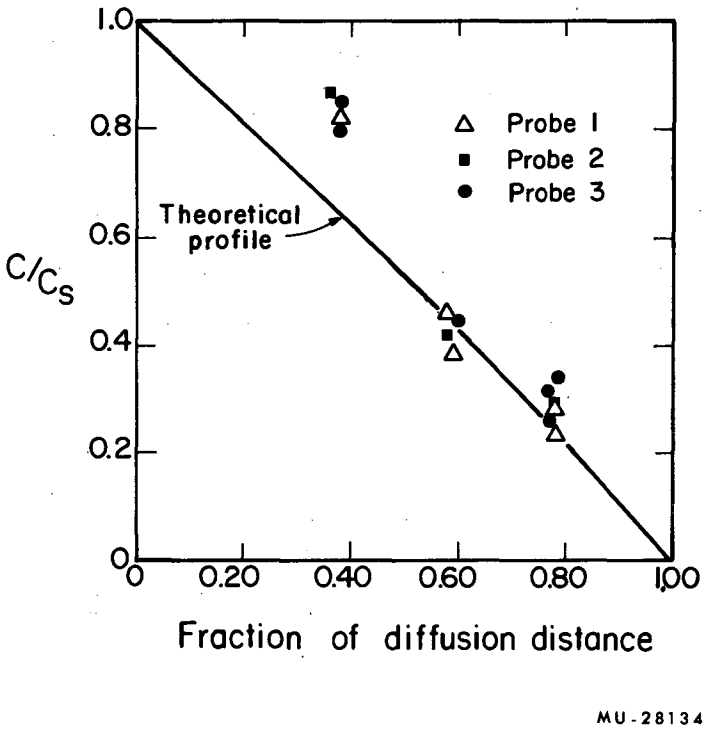

Fig. 6. Experimental concentration profile.

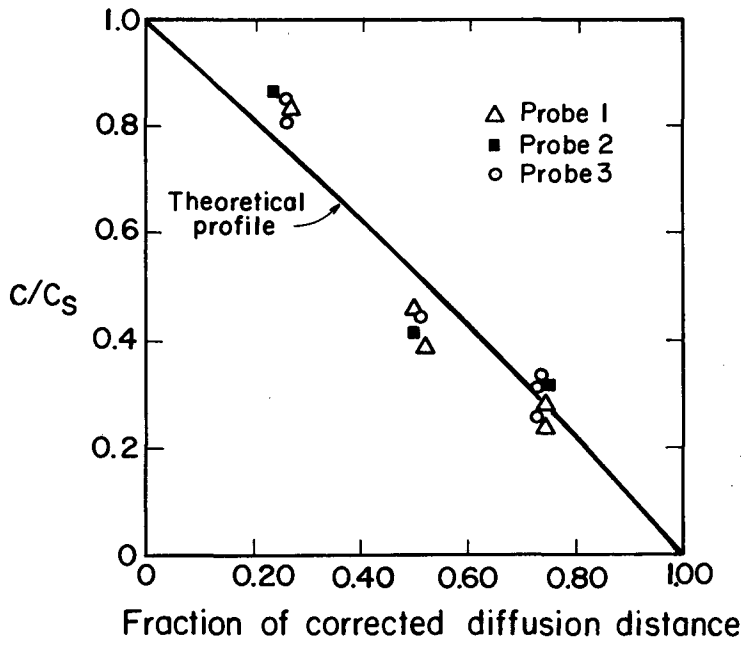

Fig. 7. Experimental concentration profile corrected for end effects.